Spectroscopy and critical temperature of diffusive superconducting/ferromagnetic hybrid structures with spin-active interfaces

Audrey Cottet
Laboratoire de Physique Théorique et Hautes Énergies, Universités Paris 6 et 7, CNRS, UMR 7589, 4 place Jussieu, F-75252 Paris Cedex 05, France
and Laboratoire de Physique des Solides, Université Paris-Sud, CNRS, UMR 8502, F-91405 Orsay Cedex, France
(Received 20 April 2007; revised manuscript received 16 July 2007; published 7 December 2007)

The description of the proximity effect in superconducting/ferromagnetic heterostructures requires use of spin-dependent boundary conditions. Such boundary conditions must take into account the spin dependence of the phase shifts acquired by electrons upon scattering on the boundaries of ferromagnets. The present article shows that this property can strongly affect the critical temperature and the energy dependence of the density of states of diffusive heterostructures. These effects should allow a better characterization of diffusive superconductor/ferromagnet interfaces.

DOI: 10.1103/PhysRevB.76.224505 PACS number(s): 74.50.+r, 74.20.−z, 73.23.−b

I. INTRODUCTION

When a ferromagnetic metal (F) with uniform magnetization is connected to a BCS superconductor (S), the singlet electronic correlations characteristic of the S phase can propagate into F because electrons and holes with opposite spins and excitation energies are coupled coherently by Andreev reflections occurring at the S/F interface. Remarkably, the ferromagnetic exchange field induces an energy shift between the coupled electrons and holes, which leads to spatial oscillations of the superconducting order parameter in F.[1,2] This effect has been observed experimentally through oscillations of the density of states (DOS) in F with the thickness of F (Ref. 3) or oscillations of the critical current I_0 through S/F/S structures[4–7] with the thickness of F or the temperature. The oscillations of I_0 have allowed to obtain π junctions,[8] i.e., Josephson junctions with $I_0<0$, which could be useful in the field of superconducting circuits.[9,10] A reentrant behavior of the superconducting critical temperature of S/F bilayers with the thickness of F has also been observed.[11] At last, some F/S/F trilayers have shown a lower critical temperature for an antiparallel alignment of the magnetizations in the two F layers as compared with the parallel alignment,[12] which should offer the possibility of realizing a superconducting spin switch.[13,14]

For a theoretical understanding of the behavior of S/F hybrid circuits, a proper description of the interfaces between the different materials is crucial. For a long time, the only boundary conditions available in the diffusive case were spin-independent boundary conditions derived for S/normal metal interfaces.[15] Recently, spin-dependent boundary conditions have been introduced for describing hybrid diffusive circuits combining BCS superconductors, normal metals, and ferromagnetic insulators.[16] These boundary conditions take into account the spin polarization of the electronic transmission probabilities through the interface considered, but also the spin dependence of the phase shifts acquired by electrons upon transmission or reflection by the interface. The first property generates widely known magnetoresistance effects.[17] The second property is less commonly taken into account. However, the spin dependence of interfacial phase shifts (SDIPS) can modify the behavior of many different types of mesoscopic circuits with ferromagnetic elements, such as those including a diffusive normal metal island,[18] a resonant system,[19,20] a Coulomb blockade system,[20–22] or a Luttinger liquid.[23] It has also been shown that the SDIPS has physical consequences in S/F hybrid systems.[16,24–30] One can note that, in some references, the SDIPS is called "spin-mixing angle" or "spin-rotation angle" (see, e.g., Refs. 24 and 26). In the diffusive S/F case, the spin-dependent boundary conditions of Ref. 16 have been applied to different circuit geometries[27–30] but the only comparison to experimental data has been performed in Ref. 29. The authors of this reference have generalized the boundary conditions of Ref. 16 to the case of metallic S/F interfaces with a superconducting proximity effect in F. They have showed that the SDIPS can induce a shift in the oscillations of the critical current of a S/F/S Josephson junction or of the DOS of a S/F bilayer with the thickness of F. Signatures of this effect have been identified in the Nb/PdNi hybrid structures of Refs. 3 and 5. Nevertheless, the problem of characterizing the SDIPS of diffusive S/F interfaces has raised little attention so far, in spite of the numerous experiments performed.

A good characterization of the properties of diffusive S/F interfaces would be necessary to better control the superconducting proximity effect in diffusive heterostructures. The present article presents other consequences of the SDIPS than that studied in Ref. 29, which could be useful in this context. In particular, the SDIPS can generate an effective magnetic field in a diffusive S in contact with a diffusive F, like found for a ballistic S in contact with a ferromagnetic insulator.[24] This effective field can be detected, in particular, through the DOS of the diffusive F layer, with a visibility which depends on the thickness of F. A strong modification of the variations of the critical temperature of diffusive S/F structures with the thickness of F is also found. These effects should allow to characterize the SDIPS of diffusive S/F interfaces through DOS and critical temperature measurements by using the heterostructures currently fabricated. The calculations reported in this paper are also appropriate to the case of a diffusive S layer contacted to a ferromagnetic insulator (FI).

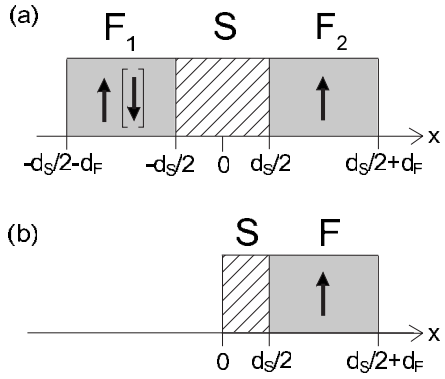

FIG. 1. (a) Diffusive F/S/F trilayer consisting of a BCS superconductor S with thickness d_S placed between two ferromagnetic electrodes F_1 and F_2 with thickness d_F. In this picture, the directions of the magnetic polarizations in F_1 and F_2 are parallel (antiparallel), which corresponds to the configuration $\mathcal{C}$=P (AP). (b) S/F bilayer consisting of a BCS superconductor S with thickness $d_S/2$ contacted to a ferromagnetic electrode F with thickness d_F.

This paper is organized as follows. Section II presents the initial set of equations used to describe the heterostructures considered. The case of F/S/F trilayers is mainly addressed, but the case of S/F (or S/FI) bilayers follows straightforwardly. Section III specializes to the case of a weak proximity effect in F and a superconducting layer with a relatively low thickness $d_S \leqslant \xi_S$, with ξ_S the superconducting coherence length in S. The spatial evolution of the electronic correlations in the S and F layers is studied in Sec. III A. The energy-dependent DOS of S/F heterostructures is calculated in Sec. III B. Section III C considers briefly the limit of S/FI bilayers. Section III D discusses SDIPS-induced effective field effects in other types of systems. Section III E compares the present work to other DOS calculations for data interpretation in S/F heterostructures. Critical temperatures of S/F circuits are calculated and discussed in Sec. III F. Conclusions are presented in Sec. IV. Throughout the paper, I consider conventional BCS superconductors with an *s*-wave symmetry.

II. INITIAL DESCRIPTION OF THE PROBLEM

This article mainly considers a diffusive F/S/F trilayer consisting of a BCS superconductor S for $-d_S/2<x<d_S/2$, and ferromagnetic electrodes F_1 for $x \in \{-d_S/2-d_F,-d_S/2\}$ and F_2 for $x \in \{d_S/2,d_S/2+d_F\}$ [see Fig. 1(a)]. The magnetic polarization of the two ferromagnets can be parallel (configuration $\mathcal{C}$=P) or antiparallel (configuration $\mathcal{C}$=AP), but the modulus $|E_{ex}|$ of the ferromagnetic exchange field is assumed to be the same in F_1 and F_2. Throughout the structure, the normal quasiparticle excitations and the superconducting condensate of pairs can be characterized with Usadel normal and anomalous Green's functions $G_{n,\sigma}=\mathrm{sgn}(\omega_n)\cos(\theta_{n,\sigma})$ and $F_{n,\sigma}=\sin(\theta_{n,\sigma})$, with $\theta_{n,\sigma}(x)$ the superconducting pairing angle, which depends on the spin direction $\sigma \in \{\uparrow,\downarrow\}$, the Matsubara frequency $\omega_n(T)=(2n+1)\pi k_B T$, and the coordinate x (see, e.g., Ref. 31). The Usadel equation describing the spatial evolution of $\theta_{n,\sigma}$ writes

$$\frac{\hbar D_S}{2}\frac{\partial^2 \theta_{n,\sigma}}{\partial x^2} = |\omega_n|\sin(\theta_{n,\sigma}) - \Delta(x)\cos(\theta_{n,\sigma}) \tag{1}$$

in S and

$$\frac{\hbar D_F}{2}\frac{\partial^2 \theta_{n,\sigma}}{\partial x^2} = (|\omega_n| + iE_{\mathrm{ex}}\sigma\ \mathrm{sgn}(\omega_n))\sin(\theta_{n,\sigma}) \tag{2}$$

in F_1 and F_2, with D_F the diffusion constant of the ferromagnets and D_S the diffusion constant of S. The self-consistent superconducting gap $\Delta(x)$ occurring in Eq. (1) can be expressed as

$$\Delta(x) = \frac{\pi k_B T \lambda}{2} \sum_{\substack{\sigma \in \{\uparrow,\downarrow\} \\ \omega_n(T) \in \{-\Omega_D,\Omega_D\}}} \sin(\theta_{n,\sigma}), \tag{3}$$

with Ω_D the Debye frequency of S, $\lambda^{-1} = 2\pi k_B T_c^{BCS} \Sigma_{\omega_n(T_c^{BCS}) \in \{0,\Omega_D\}} \omega_n^{-1}$ the BCS coupling constant, and T_c^{BCS} the bulk transition temperature of S. I assume $\Delta = 0$ in F_1 and F_2. The above equations must be supplemented with boundary conditions describing the interfaces between the different materials. First, one can use

$$\left.\frac{\partial \theta_{n,\sigma}}{\partial x}\right|_{x=\pm(d_S/2+d_F)} = 0 \tag{4}$$

for the external sides of the structure. Second, the boundary conditions at the S/F interfaces can be calculated by assuming that the interface potential locally dominates the Hamiltonian, i.e., at a short distance, it causes only ordinary scattering (with no particle-hole mixing) (see, e.g., Ref. 32). This ordinary scattering can be described with transmission and reflection amplitudes $t_{n,\sigma}^{S(F)}$ and $r_{n,\sigma}^{S(F)}$ for electrons coming from the S(F) side of the interface in channel n with a spin direction σ. The phases of $t_{n,\sigma}^{S(F)}$ and $r_{n,\sigma}^{S(F)}$ can be spin dependent due to the exchange field E_{ex} in $F_{1(2)}$ and a possible spin dependence of the barrier potential between S and $F_{1(2)}$. Boundary conditions taking into account this so-called SDIPS have been derived for $|t_{n,\uparrow}^S|^2, |t_{n,\downarrow}^S|^2 \ll 1$ and a weakly polarized F.[16,29] When there is no SDIPS, the boundary conditions involve the tunnel conductance $G_T = G_Q \Sigma_n T_n$ and the magnetoconductance $G_{MR} = G_Q \Sigma_n (|t_{n,\uparrow}^S|^2 - |t_{n,\downarrow}^S|^2)$, with $\uparrow$ ($\downarrow$) the majority (minority) spin direction in the F electrode considered, $G_Q = e^2/h$, and $T_n = |t_{n,\uparrow}^S|^2 + |t_{n,\downarrow}^S|^2$. In the case of a finite SDIPS, one must also use the conductances $G_\phi^{F(S)} = 2G_Q \Sigma_n (\rho_n^{F(S)} - 4[\tau_n^{S(F)}/T_n])$, $G_\xi^{F(S)} = -G_Q \Sigma_n \tau_n^{S(F)}$, and $G_\chi^{F(S)} = G_Q \Sigma_n T_n (\rho_n^{F(S)} + \tau_n^{S(F)})/4$, with $\rho_n^m = \mathrm{Im}[r_{n,\uparrow}^m r_{n,\downarrow}^{m*}]$ and $\tau_n^m = \mathrm{Im}[t_{n,\uparrow}^m t_{n,\downarrow}^{m*}]$ for $m \in \{S,F\}$. In the following, I will focus on the effects of G_ϕ^F and G_ϕ^S, and I will assume G_{MR}, $G_\xi^{F(S)}$, and $G_\chi^{F(S)}$ to be negligible, like with a simple barrier model in the limit $T_n \ll 1$ and $E_{ex} \ll E_F$.[29] In this case, one finds that the boundary conditions for the S/F interface located at $x=x_j = (-1)^j d_s/2$, with $j \in \{1,2\}$, write

$$\xi_F \left.\frac{\partial \theta^F_{n,\sigma}}{\partial x}\right|_{x_j} = (-1)^j \gamma_T \sin[\theta^F_{n,\sigma} - \theta^S_{n,\sigma}] + i\gamma^F_\phi \epsilon^{\mathcal{C},j}_{n,\sigma} \sin[\theta^F_{n,\sigma}] \tag{5}$$

and

$$\xi_F \left.\frac{\partial \theta^F_{n,\sigma}}{\partial x}\right|_{x_j} - \frac{\xi_S}{\gamma} \left.\frac{\partial \theta^S_{n,\sigma}}{\partial x}\right|_{x_j} = \sum_{m\in\{F,S\}} i\gamma^m_\phi \epsilon^{\mathcal{C},j}_{n,\sigma} \sin[\theta^m_{n,\sigma}], \tag{6}$$

where the indices S and F indicate whether $\theta_{n,\sigma}$ and its derivative are taken at the S or F side of the interface. These equations involve the reduced conductances $\gamma_T = G_T \xi_F / A\sigma_F$ and $\gamma^{F(S)}_\phi = G^{F(S)}_\phi \xi_F / A\sigma_F$, the barrier asymmetry coefficient $\gamma = \xi_S \sigma_F / \xi_F \sigma_S$, the superconducting coherence length scale $\xi_S = (\hbar D_S / 2\Delta_{BCS})^{1/2}$, the magnetic coherence length scale $\xi_F = (\hbar D_F / |E_{ex}|)^{1/2}$, the gap Δ_{BCS} for a bulk S, the normal state conductivity $\sigma_{F(S)}$ of the F(S) material, and the junction area A. The coefficient $\epsilon^{\mathcal{C}}_{n,j}$ takes into account the direction of the ferromagnetic polarization of electrode F_j in configuration $\mathcal{C} \in \{P, AP\}$. One can use the convention $\epsilon^{P,j}_{n,\sigma} = (-1)^j \sigma \,\mathrm{sgn}(\omega_n)$ and $\epsilon^{AP,j}_{n,\sigma} = \sigma \,\mathrm{sgn}(\omega_n)$, in which the factor $\mathrm{sgn}(\omega_n)$ arising from the definition of $\theta_{n,\sigma}$ and the terms $(-1)^j$ and σ arising from the boundary conditions have been included for compactness of the expressions. Note that in the presence of a finite SDIPS, i.e., $\gamma^{F(S)}_\phi \neq 0$, the right hand side of Eq. (6) is not zero, contrarily to what is found in the spin-degenerate case.[15] In the general case, γ^F_ϕ and γ^S_ϕ are different (see, e.g., Appendix A). This implies that, with the present approximations, each interface is characterized by three parameters: γ_T, γ^F_ϕ, and γ^S_ϕ. For the sake of simplicity, symmetric F/S/F trilayers are considered, so that γ_T, γ^F_ϕ, and γ^S_ϕ are the same for the two S/F interfaces.

Before working out the above system of equations, it is interesting to note that the angle $\theta_{n,\sigma}$ calculated in the parallel configuration $\mathcal{C}=P$ for $x>0$ also corresponds to the angle $\theta_{n,\sigma}$ expected for a S/F bilayer consisting of a superconductor S for $0<x<d_S/2$ and a ferromagnetic electrode F for $x \in \{d_S/2, d_S/2+d_F\}$ [Fig. 1(b)]. In practice, using a F/S/F geometry can allow one to obtain more information on spin effects, as shown below.

III. CASE OF A THIN SUPERCONDUCTOR AND A WEAK PROXIMITY EFFECT IN F

A. Spatial variations of the pairing angle

I will assume that the amplitude of the superconducting correlations in $F_{1(2)}$ is weak, i.e., $|\theta_{n,\sigma}| \ll 1$ for $x \in \{-d_S/2 - d_F, -d_S/2\}$ and $x \in \{d_S/2, d_S/2+d_F\}$ (hypothesis 1) so that one can develop the Usadel equation [Eq. (2)] at first order in $\theta_{n,\sigma}$. This leads to

$$\frac{\partial^2 \theta_{n,\sigma}}{\partial x^2} - \left(\frac{k^{\mathcal{C},j}_{n,\sigma}}{\xi_F}\right)^2 \theta_{n,\sigma} = 0 \tag{7}$$

in the ferromagnet F_j, with $j \in \{1,2\}$, $k^{\mathcal{C},j}_{n,\sigma} = (2[i\eta^{\mathcal{C},j}_{n,\sigma} + |\omega_n / E_{ex}|])^{1/2}$, and $\eta^{\mathcal{C},j}_{n,\sigma} = (-1)^j \epsilon^{\mathcal{C},j}_{n,\sigma}$. Combining Eqs. (4) and (7), one finds in F_j

$$\theta_{n,\sigma}(x) = \theta^F_{n,\sigma}(x_j) \frac{\cosh\left(\left[x - (-1)^j\left(d_F + \frac{d_S}{2}\right)\right] \frac{k^{\mathcal{C},j}_{n,\sigma}}{\xi_F}\right)}{\cosh\left(d_F \frac{k^{\mathcal{C},j}_{n,\sigma}}{\xi_F}\right)}. \tag{8}$$

This result together with boundary condition (5) leads to

$$\theta^F_{n,\sigma}(x_j) = \frac{\gamma_T \sin(\theta^S_{n,\sigma}(x_j))}{\gamma_T \cos(\theta^S_{n,\sigma}(x_j)) + i\gamma^F_\phi \eta^{\mathcal{C},j}_{n,\sigma} + B^{\mathcal{C},j}_{n,\sigma}}, \tag{9}$$

with $B^{\mathcal{C},j}_{n,\sigma} = k^{\mathcal{C},j}_{n,\sigma} \tanh[d_F k^{\mathcal{C},j}_{n,\sigma} / \xi_F]$. This allows one to rewrite boundary condition (6) in closed form with respect to $\theta^S_{n,\sigma}$, i.e.,

$$\xi_S \left.\frac{\partial \theta^S_{n,\sigma}}{\partial x}\right|_{x_j} = (-1)^{j+1} \mathcal{L}^{\mathcal{C}}_{j,n,\sigma} \sin[\theta^S_{n,\sigma}(x_j)] \tag{10}$$

for the S/F interface located at $x=x_j$, with

$$\frac{\mathcal{L}^{\mathcal{C}}_{j,n,\sigma}}{\gamma} = \frac{\gamma_T (B^{\mathcal{C},j}_{n,\sigma} + i\gamma^F_\phi \eta^{\mathcal{C},j}_{n,\sigma})}{\gamma_T \cos(\theta^S_{n,\sigma}) + B^{\mathcal{C},j}_{n,\sigma} + i\gamma^F_\phi \eta^{\mathcal{C},j}_{n,\sigma}} + i\gamma^S_\phi \eta^{\mathcal{C},j}_{n,\sigma}. \tag{11}$$

In the following, I will assume $|E_{ex}| \gg \Delta_{\mathrm{BCS}}$ like in most experiments, so that $k^{\mathcal{C},j}_{n,\sigma} = 1 + i\eta^{\mathcal{C},j}_{n,\sigma}$. I will also assume $d_S/\xi_S \leq 1$, so that, for the $\mathcal{C}$ configuration and $-d_S/2 < x < d_S/2$, one can use

$$\theta_{n,\sigma}(x) = \tilde{\theta}^{\mathcal{C}}_{n,\sigma} - \alpha^{\mathcal{C}}_{n,\sigma}(x/\xi_S) - \beta^{\mathcal{C}}_{n,\sigma}(x/\xi_S)^2, \tag{12}$$

with $|\theta_{n,\sigma}(x) - \tilde{\theta}^{\mathcal{C}}_{n,\sigma}| \ll 1$ (hypothesis 2). Note that although experiments are often performed in the limit of thick superconducting layers $d_S > \xi_S$, assuming $d_S \leq \xi_S$ is not unrealistic since one can obtain diffusive superconducting layers with a thickness $d_S \sim \xi_S$ (see, e.g., Ref. 33). Furthermore, using relatively low values of d_S is more favorable for obtaining efficient superconducting spin switches.[34] Hypothesis 2 allows one to develop $\sin(\theta_{n,\sigma})$ and $\cos(\theta_{n,\sigma})$ at first order with respect to $\theta_{n,\sigma} - \tilde{\theta}^{\mathcal{C}}_{n,\sigma}$ in S. Accordingly, I will neglect the space dependence of $\Delta(x)$ and assign to it the value $\Delta^{\mathcal{C}}$ in configuration $\mathcal{C}$. Note that I do not make any assumption on the value of the angle $\tilde{\theta}^{\mathcal{C}}_{n,\sigma}$, which is not necessarily close to the bulk BCS value. The coefficient $\mathcal{L}^{\mathcal{C}}_{j,n,\sigma}$ is transformed into its conjugate when the magnetic polarization of electrode F_j is reversed. Therefore, I will note $\mathcal{L}^{P}_{1,n,\sigma} = \mathcal{L}^{P(AP)}_{2,n,\sigma} = \mathcal{L}^{\sigma}_n$ and $\mathcal{L}^{AP}_{1,n,\sigma} = (\mathcal{L}^{\sigma}_n)^*$. The above assumptions lead to $\alpha^{\sigma}_{n,\sigma} = 0$,

$$\beta^P_{n,\sigma} = \frac{4\mathcal{L}^{\sigma}_n \sin(\tilde{\theta}^{\mathcal{C}}_{n,\sigma})}{4\delta_S + \cos(\tilde{\theta}^{\mathcal{C}}_{n,\sigma})\delta^2_S \mathcal{L}^{\sigma}_n}, \tag{13}$$

$$\alpha^{AP}_{n,\sigma} = i\,\mathrm{Im}[\mathcal{L}^{\sigma}_n] \frac{4\sin(\tilde{\theta}^{\mathcal{C}}_{n,\sigma}) - \cos(\tilde{\theta}^{\mathcal{C}}_{n,\sigma})\delta^2_S \beta_{AP}}{4 + 2\,\mathrm{Re}[\mathcal{L}^{\sigma}_n]\cos(\tilde{\theta}^{\mathcal{C}}_{n,\sigma})\delta_S}, \tag{14}$$

and

$$\beta_{n,\sigma}^{AP} = \frac{(8\,\mathrm{Re}[\mathcal{L}_n^\sigma] + 4|\mathcal{L}_n^\sigma|^2 \cos(\tilde{\theta}_{n,\sigma}^{\mathcal{C}})\delta_S)\sin(\tilde{\theta}_{n,\sigma}^{\mathcal{C}})}{8\delta_S + 6\,\mathrm{Re}[\mathcal{L}_n^\sigma]\cos(\tilde{\theta}_{n,\sigma}^{\mathcal{C}})\delta_S^2 + |\mathcal{L}_n^\sigma|^2 \cos^2(\tilde{\theta}_{n,\sigma}^{\mathcal{C}})\delta_S^3}, \tag{15}$$

with $\delta_S = d_S/\xi_S$. On the other hand, from Eq. (1), one finds

$$\beta_{n,\sigma}^{\mathcal{C}} = \frac{\Delta^{\mathcal{C}}\cos(\tilde{\theta}_{n,\sigma}^{\mathcal{C}}) - |\omega_n|\sin(\tilde{\theta}_{n,\sigma}^{\mathcal{C}})}{2\Delta_{BCS}}. \tag{16}$$

The comparison between Eqs. (13), (15), and (16) allows one to find $\tilde{\theta}_{n,\sigma}^{\mathcal{C}}$ as a function of $\Delta^{\mathcal{C}}$. Then, one has to calculate $\Delta^{\mathcal{C}}$ by using the self-consistency relation Eq. (3). I will study below the DOS and the critical temperature following from these equations, in a limit which leads to simple analytical expressions.

B. Low-temperature density of states of S/F heterostructures

The DOS of the ferromagnets F_1 and F_2 of Fig. 1(a) can be probed at $x = \pm(d_F + d_S/2)$ by performing tunneling spectroscopy through an insulating layer. So far, this quantity has been less measured[3,35–37] than critical temperatures or supercurrents. However, this way of probing the superconducting proximity effect is very interesting because it allows one to obtain spectroscopic information. It has been shown that the zero-energy DOS of a F layer in contact with a superconductor oscillates with the thickness of F. For certain thicknesses, this zero-energy DOS can even become higher than its normal state value N_0,[38–41] as shown experimentally in Ref. 3. Remarkably, the SDIPS can shift these oscillations.[29] Although the energy dependence of the DOS of diffusive S/F structures has raised some theoretical and experimental interest, the effect of the SDIPS on this energy dependence has not been investigated so far.

For calculating analytically the low-temperature DOS of the structure of Fig. 1(a), one can assume $\gamma_T^2\cos(\theta_{n,\sigma}^S(x_j))/|(\gamma_T\cos(\theta_{n,\sigma}^S(x_j)) + i\gamma_\phi^F\eta_{n,\sigma}^{P,2} + B_{n,\sigma}^{P,2})(\gamma_T + i\gamma_\phi^S\eta_{n,\sigma}^{P,2})| \ll 1$ (hypothesis 3), which leads to $\mathcal{L}_n^\sigma = \gamma(\gamma_T + i\gamma_\phi^S\sigma\,\mathrm{sgn}(\omega_n))$. This hypothesis is, e.g., valid for $d_F \geq \xi_F$ and any value of $\gamma_\phi^{S(F)}$ if γ_T is relatively small (see, e.g., Fig. 2). I will also assume that the lowest order terms in δ_S prevail in the numerators and denominators of expressions (13) and (15), i.e., $\beta_{n,\sigma}^P \sim \mathcal{L}_n^\sigma \sin(\tilde{\theta}_{n,\sigma}^{\mathcal{C}})\delta_S^{-1}$ and $\beta_{n,\sigma}^{AP} \sim \mathrm{Re}[\mathcal{L}_n^\sigma]\sin(\tilde{\theta}_{n,\sigma}^{\mathcal{C}})\delta_S^{-1}$ (hypothesis 4). Taking into account hypothesis 3 and $\gamma \sim 1$, hypothesis 4 is valid provided γ_T and $|\gamma_\phi^S|$ are relatively small compared to 1. Importantly, hypotheses 3 and 4 are less restrictive regarding the value of γ_ϕ^F. Accordingly, I will often use $\gamma_T, |\gamma_\phi^S| \ll |\gamma_\phi^F|$, in the figures of this paper. Hypotheses 3 and 4 lead to

$$\tilde{\theta}_{n,\sigma}^{\mathcal{C}} = \arctan\left(\frac{\Delta^{\mathcal{C}}}{|\omega_n| + \Omega_{n,\sigma}^{\mathcal{C}}}\right), \tag{17}$$

with

$$\Omega_{n,\sigma}^P = 2\Delta_{BCS}\gamma(\gamma_T + i\gamma_\phi^S\sigma\,\mathrm{sgn}(\omega_n))\delta_S^{-1} \tag{18}$$

and

$$\Omega_{n,\sigma}^{AP} = 2\Delta_{BCS}\gamma\gamma_T\delta_S^{-1}. \tag{19}$$

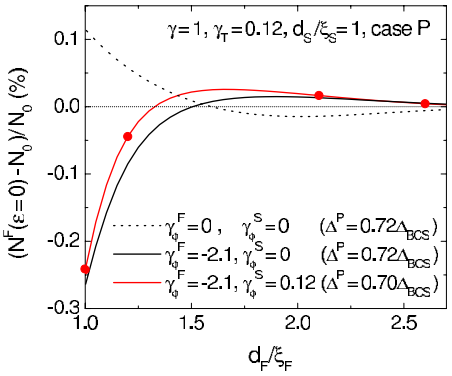

FIG. 2. (Color online) Zero-energy density of states $N^F(\varepsilon=0)$ at $x = d_F + d_S/2$ as a function of d_F for the F/S/F structure of Fig. 1(a) in the P configuration, with $\gamma=1$, $\gamma_T=0.12$, and $d_S/\xi_S=1$. The different curves correspond to different SDIPS parameters: $\gamma_\phi^F=\gamma_\phi^S=0$ (black dotted curve), $\{\gamma_\phi^F=-2.1,\ \gamma_\phi^S=0\}$ (black full curve), and $\{\gamma_\phi^F=-2.1,\ \gamma_\phi^S=0.12\}$ (red full curve). The low-temperature self-consistent gap Δ^P found for these three different cases is indicated at the bottom right of the figure. Using a strong value for γ_ϕ^F allows one to change significantly the phase of the oscillations of $N_\sigma^F(0)$ with d_F (effect similar to Ref. 29). One can check that hypotheses 1–4 are valid for the parameters used in this figure. Note that for the different cases considered here, the critical temperature T_c^P of the structure (see Sec. III F) is such that $0.615T_c^{BCS} < T_c^P < 0.635T_c^{BCS}$. The four red points correspond to the red full curves shown in Fig. 3.

Equations (17) and (18) show that an effective magnetic field H_{eff} appears in the S layer in the P configuration due to $\gamma_\phi^S \neq 0$. From Eqs. (17) and (18), H_{eff} can be expressed as

$$g\mu_B H_{eff} = \frac{\hbar v_F^S}{d_s}\frac{2G_\phi^S\ell_e^S}{3\sigma_S A} = 2E_{Th}^S\frac{G_\phi^S}{G_S}. \tag{20}$$

Here, v_F^S and ℓ_e^S denote the Fermi velocity and mean free path in S, and $G_S = \sigma_S A/d_S$ and $E_{Th}^S = \hbar D_S/d_S^2$ denote the normal state conductance and the Thouless energy of the S layer of Fig. 1(a). From Eqs. (17) and (19), the effective field effect disappears in the AP configuration because the two contacts are assumed to be symmetric and, therefore, their contributions to H_{eff} compensate each other in the AP case. Note that, in principle, the γ_ϕ^F term can induce an effective field analog to H_{eff} in the F layer, but this effect is not relevant in the regime studied in this paper (see Appendix B). The effects of H_{eff} on the DOS of the structure will be investigated in the next paragraphs. In order to calculate $\Delta^{\mathcal{C}}$, one has to combine the self-consistency relation (3) with Eq. (17), which gives, at low temperatures,

$$\mathrm{Re}\left[\log\left(\frac{\Omega_{n,\sigma}^{\mathcal{C}} + \sqrt{(\Omega_{n,\sigma}^{\mathcal{C}})^2 + (\Delta^{\mathcal{C}})^2}}{\Delta_{BCS}}\right)\right] = 0. \tag{21}$$

This equation can be solved numerically. The resulting $\Delta^{\mathcal{C}}$ is independent of the values of n and σ used in Eq. (21). Then, the value of the pairing angle $\theta_{n,\sigma}$ in the ferromagnets can be found by using Eqs. (8), (9), (12), and (17). Note that for $\gamma \ll 1$, the above equations are in agreement with formula (5) of Ref. 29, obtained with rigid boundary conditions, i.e., $\theta_{n,\sigma}$

equal to its bulk value at the S side. The energy dependence of $\theta_{n,\sigma}$ can be found by performing the analytic continuation $\omega_n=-i\varepsilon+\Gamma$ and $\mathrm{sgn}(\omega_n)=1$ in the above equations. The rate $\Gamma=0.05$ is used to account for inelastic processes.[42] At last, the density of states $N_\sigma(x,\varepsilon)$ at position x for the spin direction $\sigma\in\{\uparrow,\downarrow\}$ can be calculated by using $N_\sigma(x,\varepsilon)=(N_0/2)\mathrm{Re}[\cos[\theta_{n,\sigma}(x)]]$, where $N_0/2$ is the normal density of states per spin direction.

In the following, I will mainly focus on $N^F(\varepsilon)=\Sigma_{\sigma\in\{\uparrow,\downarrow\}}N_\sigma(x=d_F,\varepsilon)$. Figure 2 shows the variations of the zero-energy density of states $N^F(\varepsilon=0)$ as a function of d_F for interface parameters $\gamma_T=\gamma_\phi^S=0.12$ and $\gamma_\phi^F=-2.1$. Importantly, the value $\gamma_T=0.12$ seems realistic, at least for the weakly polarized $Nb/Pd_{0.9}Ni_{0.1}$ bilayers used in Ref. 3, for which one finds $\gamma_T\sim 0.15$ (see Ref. 43). In addition, a simple barrier model suggests that the situation $|G_\phi^F|\geqslant G_T$ with $G_\phi^F<0$ can happen (see Appendix A). The value $\gamma_\phi^F=-2.1$ used in Fig. 2 thus seems possible. One can see that γ_ϕ^F can change significantly the phase of the oscillations of $N^F(\varepsilon=0)$ with d_F (this effect has already been studied in Ref. 29 in the case of rigid boundary conditions but I recall it here for the sake of completeness). In Fig. 2, using for γ_ϕ^F a strong negative value allows one to get $N^F(0)<N_0$ for the lowest values of d_F, like often found in experiments. Note that from Fig. 2, γ_ϕ^S can also shift the oscillations of $N^F(\varepsilon=0)$ with d_F. Here, this effect is much weaker than that of γ_ϕ^F, but one has to keep in mind that the limit $\gamma_\phi^S\ll\gamma_\phi^F$ is considered.

Equation (20) shows that a measurement of H_{eff} should allow to determine the conductance G_ϕ^S of a diffusive S/F interface. In this context, studying the energy dependence of $N^F(\varepsilon)$ is very interesting because it can allow to see clear signatures of H_{eff}, as shown below. Figure 3 shows the energy dependence of $N^F(\varepsilon)$ in the P and AP configurations for a finite value of γ_ϕ^S and different values of d_F. For $\mathcal{C}=$P, $N^F(\varepsilon)$ shows some "double-gap" structures which disappear if the device is switched to the AP configuration. These double structures are an indirect manifestation of the effective magnetic field H_{eff} occurring in S in the P configuration due to $\gamma_\phi^S\neq 0$. Although H_{eff} is localized in the S layer, the double-gap structure that this field produces in the DOS of S is transmitted to the DOS of F due to Andreev reflections occurring at the S/F interfaces, as shown by Eq. (9). Interestingly, Rowell and McMillan have already observed that an internal property of a S layer can be seen through the superconducting proximity effect occurring in a nearby normal layer. More precisely, these authors have found that the DOS of a Ag layer can reveal the phonon spectrum of an adjacent superconducting Pb layer.[46] Remarkably, the visibility of H_{eff} in $N^F(\varepsilon)$ is modulated by quantum interferences occurring in F. Indeed, H_{eff} is more visible for certain values of d_F (e.g., $d_F/\xi_F=1.0$ or 1.2 in Fig. 3) than others (e.g., $d_F/\xi_F=2.1$ in Fig. 3), due to the d_F dependence of Eq. (9).

It is useful to note that the SDIPS-induced effective field H_{eff} should also occur in the S/F bilayer of Fig. 1(b). In this case, the Thouless energy and normal state conductance of the S layer correspond to $\tilde{E}_{Th}^S=4E_{Th}^S$ and $\tilde{G}_S=2G_S$, respectively, so that one finds $g\mu_B H_{eff}=\tilde{E}_{Th}^S G_\phi^S/\tilde{G}_S$. Double-gap structures strikingly similar to those shown in Fig. 3 were

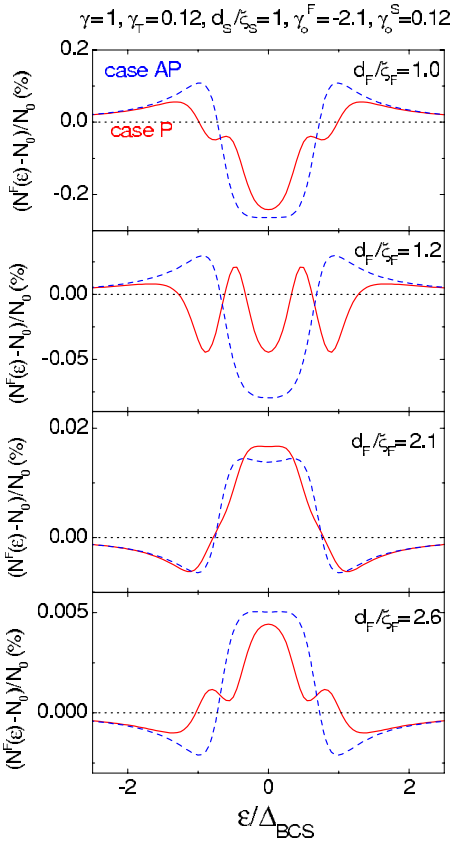

FIG. 3. (Color online) Density of states $N^F(\varepsilon)$ at $x=d_F+d_S/2$ as a function of the energy ε for the F/S/F structure of Fig. 1(a) with $\gamma=1$, $\gamma_T=0.12$, $d_S/\xi_S=1$, $\gamma_\phi^F=-2.1$, and $\gamma_\phi^S=0.12$. The different panels correspond to different values of d_F/ξ_F. The red full curves correspond to the P configuration and the blue dashed curves to the AP configuration. For finite values of γ_ϕ^S, some characteristic double-gap structures appear in $N_\sigma^F(\varepsilon)$ in the P case due to a SDIPS-induced effective field appearing in S. The visibility of this effect strongly depends on the thickness d_F of the F layers. For the different cases considered here, one can check that hypotheses 1–4 are valid and that the critical temperature $T_c^{\mathcal{C}}$ of the structure (see Sec. III F) is such that $0.62T_c^{BCS}<T_c^{\mathcal{C}}<0.67T_c^{BCS}$. Note that for the above parameters and $\gamma_\phi^S=0$, the curves obtained in the P and AP cases would be identical and very close to the AP curves shown here.

indeed measured very recently by SanGiorgio *et al.*, at the ferromagnetic side of diffusive Nb/Ni bilayers in the absence of any external magnetic field.[47] Remarkably, the visibility of the observed double structures varies with d_F, as predicted above. Note that in S/F bilayers, the field H_{eff} should also be observable directly at the S side by measuring $N^S(\varepsilon)=\Sigma_{\sigma\in\{\uparrow,\downarrow\}}N_\sigma(x=0,\varepsilon)$. However, for parameters comparable to those of Fig. 3, this should not enhance the resolution on H_{eff} (see Fig. 4, left). For certain values of d_F, H_{eff} is even more visible in $N^F(\varepsilon)$ than in $N^S(\varepsilon)$ (see Fig. 3).

Before concluding this section, I would like to emphasize that from Eqs. (17) and (19), in the AP configuration, the SDIPS-induced effective field H_{eff} disappears for the F/S/F structure considered in this paper because the two contacts are assumed to be symmetric and have thus opposite contributions to H_{eff} in the AP case. In the case of a dissymmetric

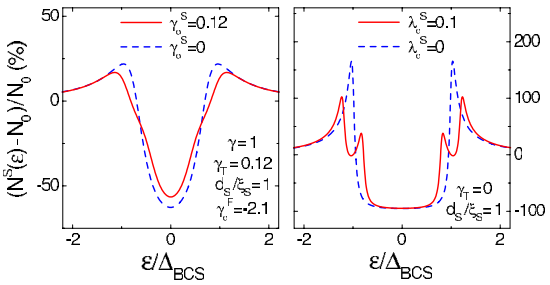

FIG. 4. (Color online) Energy dependent density of states $N^S(\varepsilon)$ measurable at the S side ($x=0$) of the S/F structure of Fig. 1(b). The left panel corresponds to the case of a metallic F contact with parameters corresponding to that of Figs. 2 and 3. In this case, the DOS measured at the S side does not allow to resolve the SDIPS-induced effective field H_{eff} better than a DOS measurement at the F side of the structure, as can be seen from a comparison with Fig. 3. For certain values of d_F, H_{eff} is even more visible in $N^F(\varepsilon)$ than in $N^S(\varepsilon)$. The right panel corresponds to the case in which F is not a metal but an insulating ferromagnet, i.e., $\gamma_T=0$. In this case, one can use the reduced SDIPS parameter $\lambda_\phi^S=G_\phi^S\xi_S/A\sigma_S$. For $\lambda_\phi^S\neq 0$, $N^S(\varepsilon)$ shows strong signatures of the effective field H_{eff} induced by the FI layer in S. One can check that hypotheses 1–4 are valid for the parameters used in this figure.

structure, this should not be true anymore, but the SDIPS-induced effective field should nevertheless vary from the P to the AP case. This is one practical advantage of working with F/S/F trilayers instead of S/F bilayers.

C. Low-temperature density of states of S/FI bilayers

Twenty years ago, internal Zeeman fields were observed in superconducting Al layers contacted to different types of FIs (see Refs. 48–51). Using a *ballistic* S/FI bilayer model, Ref. 24 suggested that the observed internal fields could be induced by the SDIPS.[24] However, the inadequacy of this ballistic approach for modeling the actual experiments was pointed out in Ref. 51. Most of the experiments on Al/FI interfaces were interpreted by their authors in terms of a diffusive approach with no SDIPS and an internal Zeeman field added arbitrarily in the Al layer (see Refs. 50–52). The calculations of Sec. III B provide a microscopic justification for the use of such an internal field in the diffusive model. Indeed, using $\gamma_T=0$ in the above calculations allows one to address the case of diffusive S/FI bilayers. One finds that the SDIPS-induced effective field H_{eff} of Eq. (20) can occur in a thin diffusive S layer contacted to a FI layer. This effective field effect can be seen, e.g., in the density of states $N^S(\varepsilon)$ of the S layer at $x=0$ (see Fig. 4, right). Remarkably, it was found experimentally[51] that H_{eff} scales with d_s^{-1}, in agreement with Eq. (20).[53]

D. Spin dependence of interfacial phase shifts induced effective fields in other types of systems

Interestingly, the SDIPS can induce effective field effects in other types of systems. First, the case of S/N/FI trilayers with a thickness d_N of normal metal N has been studied theoretically.[27,28] In this case, a conductance G_ϕ^N similar to G_ϕ^S can be introduced to take into account the SDIPS for electrons reflected by the FI layer. The N layer is subjected to an effective field $g\mu_B H'_{eff}=E_{Th}G_\phi^N/G_N$, with G_N the conductance of N. The expression of H'_{eff} is analogous to that of H_{eff} [see Eq. (20)], up to a factor of 2, which accounts for the symmetry of the F/S/F structure with respect to $x=0$ in the P configuration. Secondly, an effective field H''_{eff} defined by $g\mu_B H''_{eff}=(\hbar v_F^W/2L)(\varphi_L^\uparrow+\varphi_R^\uparrow-\varphi_L^\downarrow-\varphi_R^\downarrow)$ has been predicted for a resonant single-channel ballistic wire with length L placed between two ferromagnetic contacts,[19] with $\varphi_{L(R)}^\sigma$ the reflection phase of electrons with spin σ incident from the wire onto the left (right) contact, and v_F^W is the Fermi velocity in the wire. The expression of H''_{eff} also shows strong similarities with that of H_{eff} [see Eq. (20), middle term]. In practice, signatures of the field H''_{eff} could be identified in a carbon nanotube contacted with two ferromagnetic contacts.[22,55] The fields H_{eff}, H'_{eff}, and H''_{eff} have the same physical origin: the energies of the states localized in the central conductor of the structure depend on spin due to the spin-dependent phase shifts acquired by electrons at the boundaries of this conductor. In all cases, the DOS of the central conductor reveals the existence of the SDIPS-induced effective field only if it already presents a strong energy dependence near the Fermi energy in the absence of a SDIPS. In the F/S/F case, this energy dependence is provided by the existence of the superconducting gap in S.[56] In the S/N/FI case, it is provided by the existence of a superconducting minigap in N. At last, in the case of the ballistic wire, it is provided by the existence of resonant states in the wire.

E. Comparison between the present work and other models for data interpretation in S/F heterostructures

For characterizing the properties of S/F interfaces, one has to interpret the experimental data showing the oscillations of the density of states $N^F(\varepsilon)$ in F with the thickness d_F of F (or the oscillations of the critical current I_0 of a S/F/S Josephson with d_F). However, if one uses a simple description with spin-degenerate boundary conditions, the amplitude and the phase of these signals are not independent, which makes the agreement with experimental results impossible in most cases. The SDIPS concept can solve this problem since it produces a shift of the signal oscillations with respect to the $G_\phi^{S(F)}=0$ case. However, in many cases, the observed shifts were attributed to the existence of a magnetically dead layer (MDL) at the F side of the S/F interface (see, e.g., Refs. 3, 57, and 58). In other cases, the discrepancy between the theory and the data was solved by taking into account spin-scattering processes in the F layer (see, e.g., Ref. 6). In order to have a better insight into superconducting proximity effect experiments, one must stress the importance of estimating experimentally the MDL thickness and the spin-scattering rate. In principle, spin-scattering rates can be estimated experimentally, as was done, for instance for the CuNi alloy[59] which is frequently used in proximity effect measurements (see, e.g., Refs. 6 and 57). An experimental determination of the MDL thickness has also been performed in a few structures used to measure T_c or I_0,[60–64] but so far, this parameter has not been used for a real quantitative analysis of the data.

In some situations, a model combining the SDIPS with spin scattering and/or a MDL may be necessary. In any case, it is important to point out that descriptions based on spin-degenerate boundary conditions are, in principle, incomplete since they do not account for the effective field effect described in Sec. III B.

Before concluding this section, it is interesting to note that the effective field effect produced by G_ϕ^S in S or the phase shift of the spatial oscillations of the DOS provided by G_ϕ^F in F will remain qualitatively similar when the signs of G_ϕ^S and G_ϕ^F are changed (not shown). The sign of G_ϕ^F in the experiments of Refs. 3 and 5 could be determined from a quantitative comparison between the theory and the data.[29] Below, we present a study of the critical temperature of S/F structures which can give information on the signs of G_ϕ^S and G_ϕ^F through qualitative signatures.

F. Critical temperature of S/F heterostructures

The critical temperature of S/F hybrid structures has already been the topic of many theoretical (see, e.g., Refs. 13, 14, 34, 65, and 66) and experimental (see, e.g., Refs. 11 and 12) studies, but the effects of the SDIPS on this quantity have raised little attention so far. I show below that the SDIPS can significantly modify the critical temperatures of S/F diffusive structures. Calculating the critical temperature $T_c^{\mathcal{C}}$ of the structure of Fig. 1(a) in configuration $\mathcal{C}$ requires to consider the limit in which superconducting correlations are weak in S as well as in F (hypotheses 1 and 2 are then automatically satisfied). Equations (13), (15), and (16) then lead to

$$\tilde{\theta}_{n,\sigma}^{\mathcal{C}} = \frac{\Delta^{\mathcal{C}}}{|\omega_n| + 2\Delta_{BCS} b_{n,\sigma}^{\mathcal{C}} \delta_S^{-1}}, \tag{22}$$

with

$$b_{n,\sigma}^{P} = \frac{4\mathcal{L}_{n,\sigma}^0}{4 + \delta_S \mathcal{L}_{n,\sigma}^0}, \tag{23}$$

$$b_{n,\sigma}^{AP} = \frac{8\,\mathrm{Re}[\mathcal{L}_{n,\sigma}^0] + 4|\mathcal{L}_{n,\sigma}^0|^2 \delta_S}{8 + 6\,\mathrm{Re}[\mathcal{L}_{n,\sigma}^0]\delta_S + |\mathcal{L}_{n,\sigma}^0|^2 \delta_S^2}, \tag{24}$$

and

$$\frac{\mathcal{L}_{n,\sigma}^0}{\gamma} = \frac{\gamma_T (B_{n,\sigma}^{P,2} + i\gamma_\phi^F \sigma\, \mathrm{sgn}(\omega_n))}{\gamma_T + B_{n,\sigma}^{P,2} + i\gamma_\phi^F \sigma\, \mathrm{sgn}(\omega_n)} + i\gamma_\phi^S \sigma\, \mathrm{sgn}(\omega_n). \tag{25}$$

These equations, together with Eq. (3), lead to

$$\log\left(\frac{T_c^{BCS}}{T_c^{\mathcal{C}}}\right) = \mathrm{Re}\left[\Psi\left(\frac{1}{2} + \frac{b_{n,\sigma}^{\mathcal{C}}}{\delta_S \exp(\Gamma)} \frac{T_c^{BCS}}{T_c^{\mathcal{C}}}\right)\right] - \Psi\left(\frac{1}{2}\right), \tag{26}$$

where Γ denotes Euler's constant. The resulting $T_c^{\mathcal{C}}$ is independent of the values of n and σ used in Eq. (26). Note that in the case $\gamma_\phi^S = \gamma_\phi^F = 0$ and $\delta_S \to 0$, this equation is in agreement with Eqs. (18) and (19) of Ref. 34.

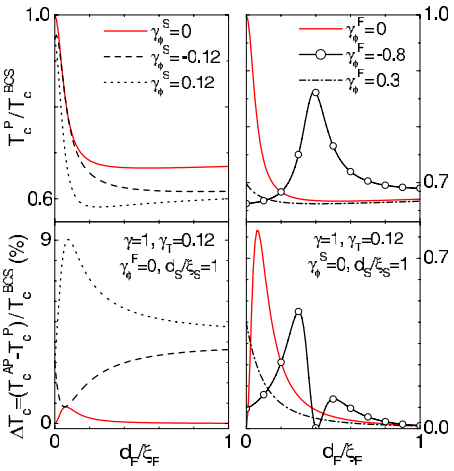

FIG. 5. (Color online) Critical temperature T_c^P for the F/S/F structure of Fig. 1(a) in the P configuration (top panels) and difference $\Delta T_c = T_c^{AP} - T_c^P$ between the critical temperatures in the P and AP configurations (bottom panels) as a function of the thickness d_F of the F layers. The left panels show the effect of a finite γ_ϕ^S and the right panels the effect of a finite γ_ϕ^F. The four panels show the case $\gamma_\phi^S = \gamma_\phi^F = 0$ with full red lines for comparison. The other parameters used in the figure are $\gamma = 1$, $\gamma_T = 0.12$, and $d_S/\xi_S = 1$. The SDIPS modifies $T_c^{\mathcal{C}}$ and ΔT_c in a quantitative or qualitative way, depending on the case considered. The type of effects produced by the SDIPS on $T_c^{\mathcal{C}}$ and ΔT_c strongly depend on the signs of γ_ϕ^F and γ_ϕ^S.

By performing a numerical resolution of Eq. (26) together with (23) and (24), one obtains the results of Fig. 5, which shows the critical temperature T_c^P of the structure in the P configuration (top panels) and the difference $\Delta T_c = T_c^{AP} - T_c^P$ (bottom panels) as a function of d_F for different interface parameters.[67] Here, for simplicity, I consider cases where $T_c^{\mathcal{C}}$ does not show a strongly reentrant behavior, i.e., a cancellation of $T_c^{\mathcal{C}}$ in a certain interval of d_F. Such a behavior can happen, for instance, for larger values of γ_T (see, e.g., Ref. 34) or $\gamma_\phi^{(S)F}$, but this corresponds to a minority[68] of the experimental observations made so far. The four panels of Fig. 5 show the case $\gamma_\phi^S = \gamma_\phi^F = 0$ with full red lines for comparison with the other cases, where the SDIPS is finite. I first comment on the results obtained for the $T_c^P(d_F)$ curves (top panels of Fig. 5). In some cases, the SDIPS can modify quantitatively the $T_c^P(d_F)$ curves, for instance, by amplifying the dip expected in $T_c^P(d_F)$ in the absence of a SDIPS (see, e.g., dotted curve in the upper left panel, corresponding to $\gamma_\phi^S > 0$). In some other cases, the SDIPS can modify qualitatively the $T_c^P(d_F)$ curves, for instance, by transforming the minimum expected in $T_c^P(d_F)$ into a maximum (see, e.g., curve with circles in the upper right panel, corresponding to $\gamma_\phi^F < 0$). I now comment on the results obtained for the $\Delta T_c(d_F)$ curves (bottom panels of Fig. 5). In the range of parameters studied in this work, one always finds $\Delta T_c > 0$ because the effects of the two F layers on S are partially compensated in the AP case. In the absence of a SDIPS and for a low γ_T, the $\Delta T_c(d_F)$ curve presents a maximum at a finite value of d_F (see red full lines in bottom panels). In some cases, the SDIPS can modify quantitatively the $\Delta T_c(d_F)$ curves, for instance, by increasing the value of this

maximum (see dotted curve in the bottom left panel, corresponding to $\gamma_\phi^S > 0$). In other cases, the SDIPS can modify qualitatively the $\Delta T_c(d_F)$ curves, for instance, by turning the maximum expected in $\Delta T_c(d_F)$ into a minimum (see dashed curve in the bottom left panel, corresponding to $\gamma_\phi^S < 0$), or by increasing the complexity of the variations of ΔT_c with d_F (see curve with circles in the bottom right panel, corresponding to $\gamma_\phi^F < 0$), or by transforming $\Delta T_c(d_F)$ into a monotonically decreasing curve with a reduced amplitude (see dot-dashed curve in bottom right panel, corresponding to $\gamma_\phi^F > 0$). Remarkably, the type of effects produced by the SDIPS on the $T_c^{\mathcal{C}}(d_F)$ and $\Delta T_c(d_F)$ curves depends on the sign of γ_ϕ^F and γ_ϕ^S. Critical temperature measurements can thus be an interesting way to determine the values of γ_ϕ^F and γ_ϕ^S. For simplicity, I have shown here results for $\gamma_\phi^F \neq 0$ and $\gamma_\phi^S \neq 0$ separately. Nevertheless, the behavior predicted for $\gamma_\phi^F \neq 0$ and $\gamma_\phi^S \neq 0$ simultaneously remain highly informative on the values of γ_ϕ^F and γ_ϕ^S. Note that if γ_ϕ^F and γ_ϕ^S are increased compared to the values used in Fig. 5, the $T_c^{\mathcal{C}}(d_F)$ curve gets some cancellation points like in Ref. 34, but the behaviors of $T_c^{\mathcal{C}}$ and ΔT_c remain, in many cases, qualitatively dependent on the signs of γ_ϕ^F and γ_ϕ^S (not shown).

Before concluding, I note that with the approximations used in Sec. III B, the electronic correlations inside S were affected by the presence of the F electrodes through the parameter γ_ϕ^S only. Consequently, the self-consistent gap $\Delta^{\mathcal{C}}$ of the S layer was independent of d_F, and it was furthermore identical for the P and AP configurations for $\gamma_\phi^S = 0$. In the present section, I have not neglected the dependence of T_c^P and T_c^{AP} on d_F and γ_ϕ^F because I have considered parameters for which hypothesis 3 is not acceptable anymore. In particular, I have used lower values for d_F.[69]

IV. CONCLUSION

This article shows that the SDIPS can have a large variety of signatures in diffusive S/F heterostructures. Reference 29 had already predicted that the SDIPS produces a phase shifting of the oscillations of the superconducting correlations with the thickness of F layers. This article shows that this is not the only consequence of the SDIPS in S/F circuits. In particular, the SDIPS can produce an effective magnetic field in a diffusive S layer contacted to a diffusive F layer. This effective field can be seen, e.g., through the DOS of the diffusive F layer, with a visibility which oscillates with the thickness of F. The SDIPS can also modify significantly the variations of the critical temperature of a S/F bilayer or a F/S/F trilayer with the thickness of F, either in a quantitative or in a qualitative way, depending on the regime of parameters considered and, in particular, the sign of the conductances G_ϕ^S and G_ϕ^F used to account for the SDIPS of the S/F interfaces. In the case of a F/S/F spin valve, this last result also holds for the thickness dependence of the difference between the critical temperatures in the parallel and antiparallel lead configurations. These effects should help determine the parameters G_ϕ^S and G_ϕ^F of diffusive S/F interfaces. The calculations shown in this paper are also appropriate to the case of thin diffusive S layers contacted to ferromagnetic insulators.

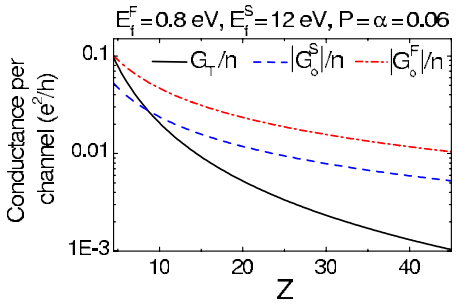

FIG. 6. (Color online) Conductances G_T (full line), $|G_\phi^S|$ (dashed lines), and $|G_\phi^F|$ (dash-dotted lines) reduced by the number of channels n as a function of the spin-averaged barrier strength Z of a S/F interface modeled with a Dirac barrier (see text). The curves were obtained with typical Fermi energies $E_f^F = 0.8$ eV and $E_f^S = 12$ eV in F and S, respectively, a spin polarization $P = 0.06$ of the density of states in F, and a spin asymmetry $\alpha = 0.06$ for the barrier. Note that for the set of parameters used in this figure, one finds $G_\phi^F < 0$ and $G_\phi^S < 0$. However, for other parameters (e.g., by using $\alpha < 0$), one can reverse the signs of G_ϕ^F and G_ϕ^S or obtain opposite signs for G_ϕ^F and G_ϕ^S (not shown).

ACKNOWLEDGMENTS

I thank P. SanGiorgio for showing me his experimental data prior to publication, which stimulated Sec. III B of this work. I acknowledge discussions with T. Kontos and W. Belzig. This work was supported by grants from the Swiss National Science Foundation and Région Ile-de-France.

APPENDIX A: PARAMETERS OF A S/F INTERFACE FROM A DIRAC BARRIER MODEL

The exact values of the conductances G_T, G_ϕ^F, and G_ϕ^S of a S/F interface depend on the details of this interface and on the microscopic structure of the contacted materials. Nevertheless, it is already interesting to study a simplified Dirac barrier model which shows that the parameter regime assumed in this paper is, in principle, possible. Neglecting the transverse part of the electron motion, one finds $r_{n,\sigma}^{S(F)} = (k_{S(F)}^\sigma - k_{F(S)}^\sigma - iZ^\sigma)/D^\sigma$ and $t_{n,\sigma}^{S(F)} = 2(k_S^\sigma k_F^\sigma)^{1/2}/D^\sigma$ with $D^\sigma = k_S^\sigma + k_F^\sigma + iZ^\sigma$. Here, $k_{S(F)}^\sigma$ is the Fermi electronic wave vector in S(F) and Z^σ is the strength of the Dirac barrier for electrons with spin σ. I use $\hbar k_S^\sigma = (2m_e E_f^S)^{1/2}$, with m_e the free electron mass and E_f^S the Fermi level in S. For F, I use an s-band Stoner model, in which $\hbar k_F^\sigma = (2m_e E_f^F[1 \pm 2P/(1+P^2)])^{1/2}$, with P the spin polarization of the density of states in F and E_f^F the Fermi level in F. I assume that the barrier can have a spin dependence $\alpha = (Z^\downarrow - Z^\uparrow)/(Z^\uparrow + Z^\downarrow)$ due to the ferromagnetic contact material used to form the interface. The results given by this approach are shown in Fig. 6. The conductances G_T, $|G_\phi^F|$, and $|G_\phi^S|$, reduced by the number of channels n, are shown as a function of the spin-averaged barrier strength $Z = (Z^\uparrow + Z^\downarrow)/2$. The three types of conductances go to zero when Z goes to infinity with α constant.[70] One can see that in the limit $T_n \ll 1$ (i.e., here $G_T h/ne^2 \ll 1$) and $P \ll 1$ in which the boundary conditions (5) and (6) have been derived, $|G_\phi^F|$ can be significantly stronger than G_T, as

assumed in Figs. 2 and 3. Note that for the set of parameters used in Fig. 6, one finds $G_\phi^F<0$ and $G_\phi^S<0$. However, for other parameters (e.g., by using $\alpha<0$), one can reverse the signs of G_ϕ^F and G_ϕ^S or obtain opposite signs for G_ϕ^F and G_ϕ^S (not shown). This suggests that there is no fundamental constraint on the signs of G_ϕ^F and G_ϕ^S in the general case.

APPENDIX B: EFFECTIVE FIELD EFFECT IN A F LAYER

This appendix reconsiders the case of the S/F bilayer of Fig. 1(b) in the limit $d_F \ll \xi_F$ where $\theta_{n,\sigma}(x)$ can be approximated with a quadratic form in the F layer. From Eqs. (2) and (5), one finds, for $x \in [d_S/2, d_S/2+d_F]$,

$$\theta_{n,\sigma}(x) = \tilde{\theta}^F_{n,\sigma} + b^F_{n,\sigma}\left[\frac{d_S-2x}{d_F} + \left(\frac{d_S-2x}{2d_F}\right)^2\right], \quad \text{(B1)}$$

with

$$\tilde{\theta}^F_{n,\sigma} = \arctan\left(\frac{\gamma_T \sin(\tilde{\theta}^S_{n,\sigma})}{\gamma_T \cos(\tilde{\theta}^S_{n,\sigma}) + \frac{2\xi_F}{d_F}\frac{\Omega_n}{E^F_{Th}} + i\gamma^F_\phi \eta^{P,2}_{n,\sigma}}\right), \quad \text{(B2)}$$

$$b^F_{n,\sigma} = \frac{\Omega_n \sin(\tilde{\theta}^F_{n,\sigma})}{E^F_{Th}}. \quad \text{(B3)}$$

$\Omega_n = |\omega_n| + iE_{ex}\eta^{P,2}_{n,\sigma}$ and $\tilde{\theta}^S_{n,\sigma} = \theta^S_{n,\sigma}(x=d_S/2)$. Here, $G_F = \sigma_F A/d_F$ and $E^F_{Th} = \hbar D_F/d_F^2$ denote the conductance and Thouless energy of the F layer (note that $d_F \ll \xi_F \Leftrightarrow E_{ex} \ll E^F_{Th}$). From completeness, I also give the analogous equations for $x \in [0, d_S/2]$. Assuming that $\theta_{n,\sigma}(x)$ can be approximated with a quadratic form in the S layer, one finds, from Eqs. (1) and (6),

$$\theta_{n,\sigma}(x) = \tilde{\theta}^S_{n,\sigma} + b^S_{n,\sigma}\left[\frac{2(2x-d_S)}{d_S} + \left(\frac{2x-d_S}{d_S}\right)^2\right], \quad \text{(B4)}$$

with

$$\tilde{\theta}^S_{n,\sigma} = \arctan\left(\frac{\gamma\gamma_T \sin(\tilde{\theta}^F_{n,\sigma}) + \frac{4\xi_S}{d_S}\frac{\Delta}{\tilde{E}^S_{Th}}}{\gamma\gamma_T \cos(\tilde{\theta}^F_{n,\sigma}) + \frac{4\xi_S}{d_S}\frac{|\omega_n|}{\tilde{E}^S_{Th}} + i\gamma\gamma^S_\phi \eta^{P,2}_{n,\sigma}}\right) \quad \text{(B5)}$$

and

$$b^S_{n,\sigma} = \frac{|\omega_n|\sin(\tilde{\theta}^S_{n,\sigma}) - \Delta\cos(\tilde{\theta}^S_{n,\sigma})}{\tilde{E}^S_{Th}}. \quad \text{(B6)}$$

The notations used in the above equations are the same as in Sec. III. In particular, the Thouless energy and the normal state conductance of the S layer with thickness $d_S/2$ are denoted $\tilde{G}_S = 2\sigma_S A/d_S$ and $\tilde{E}^S_{Th} = 4\hbar D_S/d_S^2$, and one has $\eta^{P,2}_{n,\sigma} = \sigma\,\mathrm{sgn}(\omega_n)$. In the limit $\tilde{\theta}^F_{n,\sigma} \ll 1$, Eq. (B5) is in agreement with Eqs. (17) and (18). The analytic continuation of Eq. (B5) shows that the S layer is subject to the effective field $H_{eff} = \tilde{E}^S_{Th} G^S_\phi/\tilde{G}_S$, in agreement with Eq. (20). The analytic continuation of Eq. (B2) shows that the F layer is subject to an analog effective field H^F_{eff}, defined by

$$g\mu_B H^F_{eff} = E^F_{Th}\frac{G^F_\phi}{G_F}. \quad \text{(B7)}$$

It is interesting to compare Eqs. (B2) and (9). First, note that in the regime $|\tilde{\theta}^F_{n,\sigma}| \ll 1$, Eq. (B2) can be recovered from the low d_F limit of Eq. (9). The interest of Eq. (B2) is that it is valid beyond the regime of a weak superconducting proximity effect studied in Sec. III. In particular, Eq. (B2) indicates that, in principle, the field E^F_{TH} can occur in a thin F layer for any value of the tunneling conductance G_T of the S/F interface. Interestingly, in the case of a thick F layer $d_F \geqslant \xi_F/2$, from Eq. (9), the contribution of G^F_ϕ to the pairing angle $\theta^F_{n,\sigma}(x)$ cannot be put anymore under the form of an effective exchange field due to the nonlinearity of the $B^{C,j}_{n,\sigma}$ term. Thus, strictly speaking, the concept of a SDIPS-induced effective field is valid only in the limit of thin metallic layers. However, it might be possible, in principle, to observe reminiscences of the double-gap structure appearing in $N^F(\varepsilon)$, at least in the regime of intermediate layer thicknesses $d_F \sim \xi_F$, due to the continuity of the equations. Then, one can wonder why this effect does not appear in Sec. III. This is due to the regime of parameters chosen. Sec. III assumes $E_{ex} \gg \Delta_{BCS}$ like in most experiments, and it furthermore focuses on the typical energy range probed in superconducting proximity effect measurements, i.e., $|\varepsilon| \lesssim 2\Delta_{BCS}$. In such a regime, one can neglect the term $|\omega_n|$ compared to $iE_{ex}\sigma\,\mathrm{sgn}(\omega_n)$ in Eqs. (9) and (B2), so that H^F_{eff} does not emerge in the model. Accordingly, signatures of the SDIPS-induced effective field H^F_{eff} are not likely to be observed in practice.

[1] A. I. Buzdin, L. N. Bulaevskii, and S. V. Panjukov, JETP Lett. **35**, 178 (1982).

[2] A. A. Golubov, M. Yu. Kupriyanov, and E. Il'ichev, Rev. Mod. Phys. **76**, 411 (2004).

[3] T. Kontos, M. Aprili, J. Lesueur, and X. Grison, Phys. Rev. Lett. **86**, 304 (2001).

[4] V. V. Ryazanov, V. A. Oboznov, A. Yu. Rusanov, A. V. Veretennikov, A. A. Golubov, and J. Aarts, Phys. Rev. Lett. **86**, 2427 (2001).

[5] T. Kontos, M. Aprili, J. Lesueur, F. Genêt, B. Stephanidis, and R. Boursier, Phys. Rev. Lett. **89**, 137007 (2002).

[6] H. Sellier, C. Baraduc, F. Lefloch, and R. Calemczuk, Phys. Rev. B **68**, 054531 (2003).

[7] Y. Blum, A. Tsukernik, M. Karpovski, and A. Palevski, Phys. Rev. Lett. **89**, 187004 (2002).

[8] W. Guichard, M. Aprili, O. Bourgeois, T. Kontos, J. Lesueur, and

P. Gandit, Phys. Rev. Lett. **90**, 167001 (2003).
[9] L. B. Ioffe, V. B. Geshkenbein, M. V. Feigel'man, A. L. Fauchère, and G. Blatter, Nature (London) **398**, 679 (1999).
[10] T. Yamashita, K. Tanikawa, S. Takahashi, and S. Maekawa, Phys. Rev. Lett. **95**, 097001 (2005).
[11] J. S. Jiang, D. Davidovic, D. H. Reich, and C. L. Chien, Phys. Rev. Lett. **74**, 314 (1995); L. V. Mercaldo, C. Attanasio, C. Coccorese, L. Maritato, S. L. Prischepa, and M. Salvato, Phys. Rev. B **53**, 14040 (1996).
[12] G. Deutscher and F. Meunier, Phys. Rev. Lett. **22**, 395 (1969); J. Y. Gu, C.-Y. You, J. S. Jiang, J. Pearson, Ya. B. Bazaliy, and S. D. Bader, *ibid.* **89**, 267001 (2002); A. Potenza and C. H. Marrows, Phys. Rev. B **71**, 180503(R) (2005); Ion C. Moraru, W. P. Pratt, Jr., and N. O. Birge, Phys. Rev. Lett. **96**, 037004 (2006); Phys. Rev. B **74**, 220507(R) (2006).
[13] P. G. de Gennes, Phys. Lett. **23**, 10 (1966).
[14] L. R. Tagirov, Phys. Rev. Lett. **83**, 2058 (1999); A. I. Buzdin, A. V. Vedyayev, and N. V. Ryzhanova, Europhys. Lett. **48**, 686 (1999).
[15] M. Yu. Kuprianov and V. F. Lukichev, Sov. Phys. JETP **67**, 1163 (1988).
[16] D. Huertas-Hernando, Yu. V. Nazarov, and W. Belzig, e-print arXiv:cond-mat/0204116; D. Huertas-Hernando, Ph.D. thesis, Delft University of Technology, 2002.
[17] M. N. Baibich, J. M. Broto, A. Fert, F. Nguyen Van Dau, F. Petroff, P. Etienne, G. Creuzet, A. Friederich, and J. Chazelas, Phys. Rev. Lett. **61**, 2472 (1988); G. Binasch, P. Grünberg, F. Saurenbach, and W. Zinn, Phys. Rev. B **39**, 4828 (1989).
[18] A. Brataas, Y. V. Nazarov, and G. E. W. Bauer, Phys. Rev. Lett. **84**, 2481 (2000); D. H. Hernando, Y. V. Nazarov, A. Brataas, and G. E. W. Bauer, Phys. Rev. B **62**, 5700 (2000); A. Brataas, Y. V. Nazarov, and G. E. W. Bauer, Eur. Phys. J. B **22**, 99 (2001).
[19] A. Cottet, T. Kontos, W. Belzig, C. Schönenberger, and C. Bruder, Europhys. Lett. **74**, 320 (2006).
[20] A. Cottet, T. Kontos, S. Sahoo, H. T. Man, M.-S. Choi, W. Belzig, C. Bruder, A. F. Morpurgo, and C. Schönenberger, Semicond. Sci. Technol. **21**, S78 (2006).
[21] W. Wetzels, G. E. W. Bauer, and M. Grifoni, Phys. Rev. B **72**, 020407(R) (2005); **74**, 224406 (2006).
[22] A. Cottet and M.-S. Choi, Phys. Rev. B **74**, 235316 (2006).
[23] L. Balents and R. Egger, Phys. Rev. B **64**, 035310 (2001); S. Koller, L. Mayrhofer, and M. Grifoni, New J. Phys. **9**, 348 (2007).
[24] T. Tokuyasu, J. A. Sauls, and D. Rainer, Phys. Rev. B **38**, 8823 (1988).
[25] A. Millis, D. Rainer, and J. A. Sauls, Phys. Rev. B **38**, 4504 (1988).
[26] M. Fogelström, Phys. Rev. B **62**, 11812 (2000); J. C. Cuevas and M. Fogelström, *ibid.* **64**, 104502 (2001); M. Eschrig, J. Kopu, J. C. Cuevas, and G. Schön, Phys. Rev. Lett. **90**, 137003 (2003); J. Kopu, M. Eschrig, J. C. Cuevas, and M. Fogelström, Phys. Rev. B **69**, 094501 (2004); E. Zhao, T. Löfwander, and J. A. Sauls, *ibid.* **70**, 134510 (2004); M. Eschrig, T. Löfwander, T. Champel, J. C. Cuevas, J. Kopu, and Gerd Schön, J. Low Temp. Phys. **147**, 457 (2007).
[27] D. Huertas-Hernando, Y. V. Nazarov, and W. Belzig, Phys. Rev. Lett. **88**, 047003 (2002).
[28] D. Huertas-Hernando and Yu. V. Nazarov, Eur. Phys. J. B **44**, 373 (2005).
[29] A. Cottet and W. Belzig, Phys. Rev. B **72**, 180503(R) (2005).
[30] V. Braude and Yu. V. Nazarov, Phys. Rev. Lett. **98**, 077003 (2007).
[31] N. B. Kopnin, *Theory of Nonequilibrium Superconductivity* (Clarendon, Oxford, 2001); W. Belzig, F. K. Wilhelm, C. Bruder, G. Schön, and A. D. Zaikin, Superlattices Microstruct. **25**, 1251 (1999).
[32] Yu. V. Nazarov, Superlattices Microstruct. **25**, 1221 (1999).
[33] V. Fominov, N. M. Chtchelkatchev, and A. A. Golubov, JETP Lett. **74**, 96 (2001).
[34] I. Baladié and A. Buzdin, Phys. Rev. B **67**, 014523 (2003).
[35] T. Kontos, M. Aprili, J. Lesueur, X. Grison, and L. Dumoulin, Phys. Rev. Lett. **93**, 137001 (2004).
[36] L. Crétinon, A. K. Gupta, H. Sellier, F. Lefloch, M. Fauré, A. Buzdin, and H. Courtois, Phys. Rev. B **72**, 024511 (2005).
[37] S. Reymond, P. SanGiorgio, M. R. Beasley, J. Kim, T. Kim, and K. Char, Phys. Rev. B **73**, 054505 (2006).
[38] A. Buzdin, Phys. Rev. B **62**, 11377 (2000); I. Baladié and A. Buzdin, *ibid.* **64**, 224514 (2001).
[39] M. Zareyan, W. Belzig, and Yu. V. Nazarov, Phys. Rev. Lett. **86**, 308 (2001).
[40] F. S. Bergeret, A. F. Volkov, and K. B. Efetov, Phys. Rev. B **65**, 134505 (2002).
[41] T. Yokoyama, Y. Tanaka, and A. A. Golubov, Phys. Rev. B **72**, 052512 (2005).
[42] W. Belzig, Ph.D. thesis, Karlsruhe University, 1999.
[43] In practice, the conductance G_T of a S/F interface can be very high (even for $T_n \ll 1$) and it can thus be very difficult to determine it from a normal state transport measurement. In this case, an indirect determination of G_T must be realized. In Ref. 35, Kontos *et al.*, have studied Nb/Pd bilayers with a thickness $d_{\mathrm{Pd}}=5$ nm of Pd and an interface area $A=100\times100$ μm^2. They have found from minigap measurements (Ref. 45) that the conductance G_T of their Nb/Pd interfaces was such that $\gamma_B = A\sigma_N/G_T d_{\mathrm{Nb}}=5.3$, i.e., $A\sigma_N/G_T=26.5$ nm. In Ref. 3, Kontos *et al.*, have studied Nb/$Pd_{0.9}Ni_{0.1}$ bilayers with the same interface area as for the previous Nb/Pd bilayers. The two types of bilayers were realized with the same sources of Nb and Pd and similar fabrication processes. Considering that only 10% of Ni were added to the Pd material in the S/F case, the conductivity of $Pd_{0.9}Ni_{0.1}$ was probably of the same order as that of Pd, and the conductance of the Nb/Pd interface was probably of the same order as that of Nb/$Pd_{0.9}Ni_{0.1}$. This leads to $A\sigma_F/G_T \sim 26.5$ nm. Then, using the value $\xi_F \sim 4$ nm found in Refs. 3 and 44 for $d_{\mathrm{Pd_{0.9}Ni_{0.1}}}=8$ nm, one finds $\gamma_T = G_T\xi_F/A\sigma_F \sim 0.15$.
[44] T. Kontos, Ph.D. thesis, Université Paris-Sud, 2002.
[45] The width of the minigap appearing in the density of states of a S/N bilayer versus energy gives a direct access to the parameter γ_T of this interface, as explained in A. Golubov and M. Yu. Kuprianov, Sov. Phys. JETP **69**, 805 (1989).
[46] J. M. Rowell and W. L. McMillan, Phys. Rev. Lett. **16**, 453 (1966).
[47] Paul SanGiorgio *et al.* (in preparation).
[48] P. M. Tedrow, J. E. Tkaczyk, and A. Kumar, Phys. Rev. Lett. **56**, 1746 (1986).
[49] R. Meservey and P. M. Tedrow, Phys. Rep. **238**, 173 (1994).
[50] J. S. Moodera, X. Hao, G. A. Gibson, and R. Meservey, Phys. Rev. Lett. **61**, 637 (1988); X. Hao, J. S. Moodera, and R. Meservey, Phys. Rev. B **42**, 8235 (1990).
[51] X. Hao, J. S. Moodera, and R. Meservey, Phys. Rev. Lett. **67**,

1342 (1991).
[52] J. A. X. Alexander, T. P. Orlando, D. Rainer, and P. M. Tedrow, Phys. Rev. B **31**, 5811 (1985).
[53] The fact that H_{eff} scales with d_s^{-1} is also in agreement with Eq. (1) of Ref. 13, proposed by de Gennes from Cooper's argument (Ref. 54).
[54] L. N. Cooper, Phys. Rev. Lett. **6**, 689 (1961); P. G. de Gennes, Rev. Mod. Phys. **36**, 225 (1964).
[55] S. Sahoo, T. Kontos, J. Furer, C. Hoffmann, M. Graber, A. Cottet, and C. Schönenberger, Nat. Phys. **1**, 99 (2005).
[56] Without superconductivity, H_{eff} would not be not resolvable anymore in the S/F structures considered in this paper, since it was assumed implicitly that the normal state DOS of these structures is constant near the Fermi level.
[57] V. A. Oboznov, V. V. Bol'ginov, A. K. Feofanov, V. V. Ryazanov, and A. I. Buzdin, Phys. Rev. Lett. **96**, 197003 (2006).
[58] M. Weides, M. Kemmler, E. Goldobin, D. Koelle, R. Kleiner, H. Kohlstedt, and A. Buzdin, Appl. Phys. Lett. **89**, 122511 (2006).
[59] W. P. Pratt, Jr. (private communication); see also S.-Y. Hsu, P. Holody, R. Loloee, J. M. Rittner, W. P. Pratt, Jr., and P. A. Schroeder, Phys. Rev. B **54**, 9027 (1996).
[60] Th. Mühge, N. N. Garif'yanov, Yu. V. Goryunov, G. G. Khaliullin, L. R. Tagirov, K. Westerholt, I. A. Garifullin, and H. Zabel, Phys. Rev. Lett. **77**, 1857 (1996).
[61] J. Aarts, J. M. E. Geers, E. Brück, A. A. Golubov, and R. Coehoorn, Phys. Rev. B **56**, 2779 (1997).
[62] J. W. A. Robinson, S. Piano, G. Burnell, C. Bell, and M. G. Blamire, Phys. Rev. Lett. **97**, 177003 (2006).
[63] S. Piano, J. W. A. Robinson, G. Burnell, and M. G. Blamire, Eur. Phys. J. B **58**, 123 (2007).
[64] C. Bell, R. Loloee, G. Burnell, and M. G. Blamire, Phys. Rev. B **71**, 180501(R) (2005).
[65] E. A. Demler, G. B. Arnold, and M. R. Beasley, Phys. Rev. B **55**, 15174 (1997); M. G. Khusainov and Yu. N. Proshin, *ibid.* **56**, R14283 (1997); L. R. Tagirov, Physica C **307**, 145 (1998); Yu. N. Proshin and M. G. Khusainov, JETP **86**, 930 (1998); Ya. V. Fominov, N. M. Chtchelkatchev, and A. A. Golubov, Phys. Rev. B **66**, 014507 (2002); A. Bagrets, C. Lacroix, and A. Vedyayev, *ibid.* **68**, 054532 (2003).
[66] C.-Y. You, Ya. B. Bazaliy, J. Y. Gu, S.-J. Oh, L. M. Litvak, and S. D. Bader, Phys. Rev. B **70**, 014505 (2004).
[67] With the parameters of Fig. 5, the approximations $b^P_{n,\sigma}=\mathcal{L}^0_{n,\sigma}$ and $b^{AP}_{n,\sigma}=\mathrm{Re}[\mathcal{L}^0_{n,\sigma}]$ used in Ref. 34 would be sufficient for calculating the T_c^P and T_c^{AP} curves, but not the difference ΔT_c. Indeed, for the different cases studied in this figure, the relative difference between the results obtained with these approximations and those given by Eqs. (23) and (24) is smaller than $\sim 0.8\%$ for T_c^P and T_c^{AP}, but it can reach $\sim 18\%$ for ΔT_c. This is why I have used the general equations (23) and (24) for plotting Fig. 5.
[68] L. R. Tagirov, I. A. Garifullin, N. N. Garifyanov, S. Ya. Khlebnikov, D. A. Tikhonov, K. Westerholt, and H. Zabel, J. Magn. Magn. Mater. **240**, 577 (2002).
[69] Note that both regimes $d_F \leqslant \xi_F$ (see, e.g., Ref. 36) and $d_F \geqslant \xi_F$ (see e.g., Ref. 66) seem to be accessible in practice.
[70] For $Z \to +\infty$, $G_\phi^{F(S)}$ vanishes because $\arg(r_{n,\sigma}^{F(S)}) \to \pi$ and $\arg(t_{n,\sigma}^{F(S)}) \to -\pi/2$ for $\sigma \in \{\uparrow, \downarrow\}$.